Effects of the Charging Mass of Working Fluid on the Thermal Performance of Heat Pipe with Axially Grooved Wick

Jeong-Se Suh†, Chang Ho Kang, Jung Kyu Hong

Department of Mechanical Engineering, ReCAPT, GyeongSang National University, Jinju 660-701, Korea

Key words: Heat pipe, Axial groove, Meniscus, Capillary pressure, Charging mass of working fluid, Elevation

ABSTRACT: An analytical and experimental study has been conducted to determine the optimal charging mass of working fluid for the maximum heat transport capacity of heat pipe with axially grooved wick. When the heat pipe is operated in a steady state, the liquid-vapor meniscus recession of working fluid to the bottom of groove is occurred in the evaporator region. In this work, the optimal charging mass of working fluid was obtained by considering the meniscus recession from the axial variation of capillary pressure, the radius of curvature and wetting angle of meniscus of liquid-vapor interface. Experimental results were also obtained by varying the charging mass of working fluid within a heat pipe, and presented for the trend of maximum heat transport capacity corresponding to the operating temperature and the elevation of heat pipe. Finally, the analytical results of the optimal charging mass of working fluid were compared with those from the experiment, both of which were in good agreement with each other.

1. Introduction

Heat pipe has been much regarded as heat transfer device because of ease of manufacturing due to its simplicity of structure, and it can transfer much quantity of heat with small temperature difference due to little thermal resistance. Since heat pipe with axially grooved type wick uses the open rectangular channel as a liquid passage, it has very low frictional coefficient for liquid flow compared to screen wick and also very low thermal resistance through evaporator and condenser of heat pipe because of using metal fin between grooves which has the thermal property of a pipe. Since grooved wick attached on pipe wall is also safe in the device of high pressure and long time usage, recently many types of heat pipes with axially grooved wicks have been very widely applied in the industrial field. A heat pipe with axially grooved wicks has been especially used in the field of spacecraft industry. Since space industry such as a satellite requires not only high density heat transfer characteristic but also structural simplicity and safety, A heat pipe with axially grooved wicks is generally suitable for satellite. And it is also used in the wide areas such as high precision machines, energy related industry and cooling of electric and electronic devices.

Recently, many of researches have been made to investigate the thermal characteristic of heat pipe. A survey of literatures reveals that most of researches have been focused on the improvement of heat transport capacity of heat pipe. In some of representative studies, Kemme[1]

† Corresponding author
Tel.: +82-55-751-5312; fax: +82-55-757-5622
E-mail address: jssuh@gsnu.ac.kr

reviewed the operation limitation of heat pipe and verified several types of capillary limit. Tathgir et al.[2] studied the variation of heat transfer corresponding to the charging quantity of working fluid for a stainless steel heat pipe with axially grooved wick which uses water as a working fluid. Ogushi et al.[3] studied capillary limitation and heat transfer rate of condenser with the charging mass of working fluid and the inclination angle of grooved aluminum heat pipe using Freon as a working fluid, and Shin[4] experimentally studied the optimal charging mass of working fluid of heat pipe with screen mesh wick and studied the heat transfer characteristics of heat pipe for solar heating system in the parameter of an elevation of condenser, the charging mass of working fluid, and the flow rate of cooling water of heat pipe. The heat transport capacity of heat pipe with axially grooved wicks has also been studied experimentally for various conditions of elevation and heat load.[5,6]

Otherwise, Thermal performance of heat pipe is commonly dependent on the wick structure and the charging mass of working fluid. If the mass of working fluid is charged insufficiently into the heat pipe, the dry-out phenomena happen in the evaporator region. If the charging mass of working fluid is overplus, this may lead to diminish heat transfer rate through heat pipe because of condenser blockage by the liquid slug. Thus the charging mass of working fluid is properly required to maintain optimal operation states.

In this work, the optimal charging mass of working fluid will be experimentally and analytically determined for the heat pipe with axially grooved wick. The charging mass of working fluid will be optimally determined by considering the recession of liquid-vapor interface of working fluid in a groove of the evaporator region,[4] different of the previous method.[7] Additionally, the distribution of capillary pressure, radius of curvature and wetting angle with the aid of the proposed model will also obtained from analytical solution.

2. Experiments

2.1 Experimental apparatus

Figure 1 shows a schematic diagram of experimental apparatus which is used in this study and includes the controller to maintain temperature conditions for the condenser and evaporator of heat pipe. The heat pipe used in this study consists of an evaporator, an adiabatic part and a condenser. The wall temperature of heat pipe is measured from the thermocouples attached on it and saved to a data logger. The condenser part of heat pipe is cooled using the counter-flow type heat exchanger by the circulation cooling methanol liquid from the constant temperature bath. The elevation of heat pipe is established from the horizontal holder. The adiabatic part of heat pipe is covered by a asbestos fiber overlapped with glass wool to reduce the heat loss to the surrounding. The axial block heater is attached to supply heat to the evaporator of heat pipe and controlled by the variable voltage through

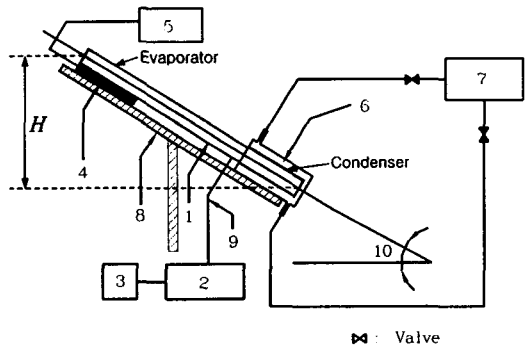

1. Heat pipe
2. Data acquisition device
3. Personal computer
4. Block heater
5. Slidacs
6. Heat sink
7. Bath circulator
8. Angle plate
9. Thermocouple
10. Inclination angle

Fig. 1 Schematic of an experimental apparatus.

Table 1 Specifications of a heat pipe used in this study

Properties	Values
Pipe material	Aluminium
Working fluid	Ammonia
Groove width (w)	0.46 mm
Base groove width	0.97 mm
Vapor core diameter (D_v)	7.43 mm
Groove depth (δ)	1.05 mm
Number of grooves (N)	21
Groove wick porosity (ε)	0.363
Cross section area of heat pipe	$11.68 \times 14.73\ mm^2$
Condenser length (L_c)	300 mm
Adiabatic length (L_a)	449 mm
Evaporator length (L_e)	140 mm

transformer. The thermal contact resistance between pipe wall and block heat is reduced by using thermal grease. The inclination angle of heat pipe is fixed up by using a horizontal gauge and a socket wrench during experiment for heat pipe. The T-type thermocouples are attached to the wall of heat pipe by thermal glue to reduce thermal resistance between thermocouple and the wall of heat pipe. Five thermocouples are set up on the evaporator, the adiabatic and condenser parts of heat pipe, respectively. It is confirmed that the deviation of temperature data between data logger and thermocouple junction are in accuracy within 0.2~0.5℃ on experimental procedure. The material of heat pipe enclosure is aluminium and the working fluid the ammonia of purity 99.9%. The specification of the axially grooved heat pipe is detailedly shown in Table 1.

2.2 Experimental procedures

Experiment for thermal performance of heat pipe is made on the charging mass of working fluid, the inclination angle and the imposed heat flow and the temperature of heat pipe wall measured. The operating temperature is regarded for the average of adiabatic part of heat pipe[8] and maintained constantly by cooling the condenser part of heat pipe for the increasing heat load. When the heat pipe reaches on the capillary limitation, the temperature increases rapidly at the evaporator of heat pipe, which becomes to be dried out. At this point, the heat transport flow rate of heat pipe can be regarded as maximum. For the other charging mass of working fluid, the above mentioned processes are also applied for the heat pipe mode which the evaporator is vertically lied above the condenser.

3. Optimal charging mass

Generally, the charging mass of working fluid is determined by considering only a geometrical shape condition as follows,[7]

$$m_{th} = A_v L_t \rho_v + A_w L_t \varepsilon \rho_l \qquad (1)$$

where A_v and A_w are the cross sectional areas of vapor core and grooves, L_t the length of heat pipe, ε the porosity of wick and ρ_v and ρ_l the densities of vapor and liquid, respectively. The charging mass of working fluid is actually required less than that from ideal condition owing to the meniscus recession of working fluid in the liquid-vapor interface. Feldman et al.[9] suggested that curvature radius became to be small by the reduced amount of liquid as the liquid-vapor interface moves toward to the bottom of grooved wick by liquid evaporation in the evaporator region but almost approaches to flat by condensing in the condenser region. Figure 2(b) describes the recession of meniscus of working fluid in operation by capillary pressure. The curvature radius is axially changed by the variation of pressure difference. Based on the axial variation of capillary pressure difference between liquid and vapor which can be obtained from the conservation equations of mass, momentum and energy,[7] the curvature

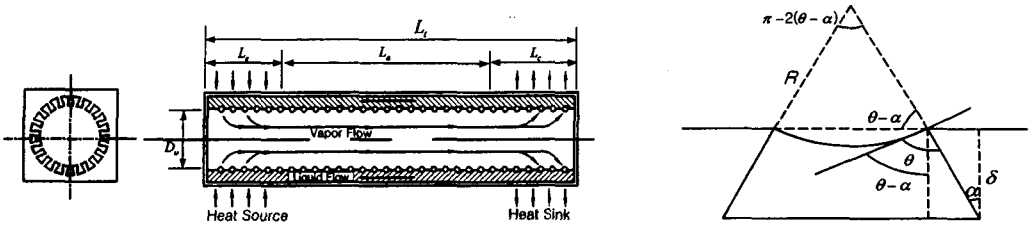

(a) Dimensions and cross section of heat pipe (b) Enlarged section of groove filled with liquid

Fig. 2 Schematic diagram of heat pipe.

radius can be calculated from Laplace-Young equation, $\Delta P(x)=1/R(x)$ and the wetting angle (θ) of liquid working fluid in a groove can be also determined by following equation.

$$\theta(x) = \cos^{-1}\left(\frac{w\Delta P(x)}{2\sigma}\right)+\alpha \qquad (2)$$

where $\Delta P(x)$ is a pressure difference between liquid and vapor, w width of a groove, σ surface tension force, α angle of groove and x axially coordinate of heat pipe, respectively. As shown in Fig. 2, the charging mass of working fluid removed from groove by capillary pressure difference is the cross sectional area of nail subtracting the triangle area from the cross sectional area of sector. The optimal charging mass of working fluid can therefore be calculated by following equation.

$$m_{opt} = m_{th} - m_{void} \qquad (3)$$

where

$$m_{void} = NV_{void}(\rho_l - \rho_v) \qquad (4)$$

$$V_{void} = \int_0^{L_t} \frac{1}{2} R(x)\{R(x)[\pi-2(\theta(x)-\alpha)] - w\sin(\theta(x)-\alpha)\}dx \qquad (5)$$

4. Results and discussion

4.1 Experimental results

Experiment has been performed to investigate the thermal performance of axially grooved heat pipe for several mass quantities of charged working fluid, m=7.3 g, 8.5 g and 8.9 g. Additionally, the influence of elevation has been experimentally investigated for several selected heights of H=0 mm, 5 mm and 10 mm to evaluate the heat transport capability of heat pipe operating in the heat pipe mode in which the evaporator is lied vertically above the condenser.

Figure 3 shows the axial distributions of wall surface temperatures of heat pipe for several heat transport capacities for typical charging mass of working fluid, m=7.3 g and 8.5 g at T_{opr}=293 K and H=0 mm. The evaporator is left of figure, the adiabatic in center, and the condenser in right. The evaporator is from 0 m to 0.14 m, the adiabatic from 0.14 m to 0.589 m, and the condenser from 0.589 m to 0.889 m. It is shown in the figure that, although the difference temperature between evaporator and condenser is small for the low heat load imposed on the heat, the temperature of evaporator increases linearly with the head load and rapidly over the critical heat load. The temperatures of condenser vary smaller than those of evaporator and decrease linearly in a different fashion of evaporator. This decreasing temperature of condenser is due to the dropped cooling temperature to maintain the constant adiabatic temperature for the increasing heat load during operating the heat pipe. It is also found that, as the heat load imposed on the evaporator of heat pipe approaches to the limitation of heat

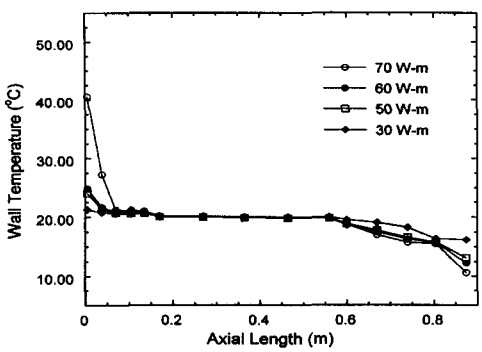

(a) m=7.3 g

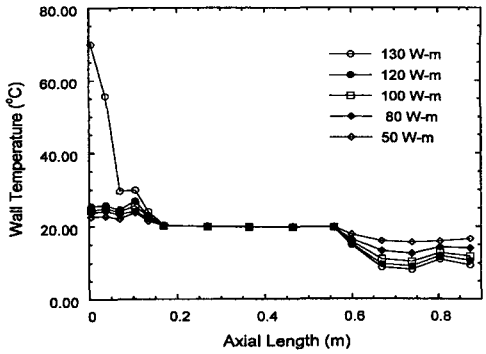

(b) m=8.5 g

Fig. 3 Wall temperature distributions for the operating temperature of 293 K at H=0 mm.

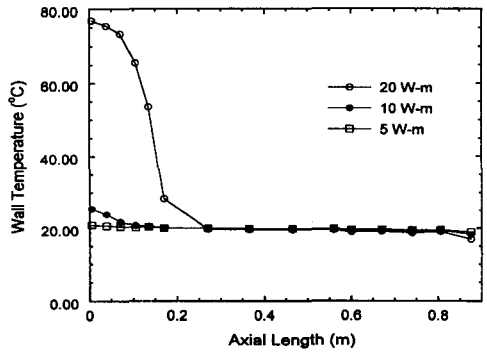

(a) m=7.3 g

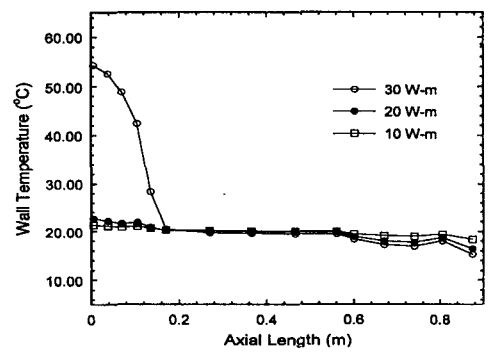

(b) m=8.5 g

Fig. 4 Wall temperature distributions for the operating temperature of 293 K at H=10 mm.

transport capacity of heat pipe, the dry-out of liquid occurs at the end of evaporator and the wall temperature of evaporator is suddenly high due to no heat transfer through pipe. For the case of m=7.3 g, the dry-out in the evaporator is occurred at the heat transport capacity of 70 Wm as shown in Fig. 3(a). For the case of m=8.5 g, Fig. 3(b) shows that the dry-out at the evaporator is occurred at the heat transport capacity(QL) of 130 Wm. It is therefore found that the charging mass of working fluid influences considerably the heat transport capacity of heat pipe. The wall temperatures in the end of condenser drop suddenly in m=7.3 g as shown in Fig. 3(a), whereas the wall temperatures drop entirely throughout the condenser in m=8.5 g as shown in Fig. 3(b). This temperature drop at the condenser of heat pipe arises from the reduction of heat reject to the surrounding due to the increasing of thermal resistance from the overflowing of working fluid to the condenser, which results in the increasing of temperature at the evaporator. This phenomena is clearly obvious with the increasing of heat transport capacity imposed on heat pipe.

Figure 4 shows the axial distribution of wall temperatures for several heat loads at the operating temperature of 293 K and the elevation of 10 mm. It is found in the figure that the dry-out at the evaporator occurs for m=7.3 g at the heat transport capacity of 20 Wm and for m=8.5 g at the heat transport capacity of

30 Wm. As shown in H=0 mm, the tendency to increase the heat transport capacity appears in H=10 mm as the mass of working fluid becomes to be charged. This behavior arises from the suppression of dry-out occurred at the evaporator of heat pipe due to the over-flowing of working fluid.

Otherwise, as compared with H=10 mm and 0 mm from Fig. 3 and Fig. 4, it is found that the heat transport capacity of heat pipe is considerably reduced with the elevation increasing. The reduction of heat transport capacity is caused by declining the returned liquid working fluid induced by the capillary forces from grooved wick due to the inverse gravity force with the elevation of condenser increasing.

Figure 5 shows the maximum heat transport capacity of heat pipe at the operating temperature 293 K for several elevations H=0 mm, 5 mm and 10 mm. In figure, symbols denote the experimental results and lines the cubic spline fitting. This figure reveals that, for H=0 mm and 5 mm, the maximum heat transport capacity ascends with the charging mass of working fluid increasing and descends over the charging mass 0.0085 kg. The optimal charging mass of working fluid can therefore be determined near m=8.5 g for H=0 mm and 5 mm. For H=10 mm, the maximum heat transport capacity continuously ascends with the charging mass of working fluid increasing in a range of experiment. It is therefore inferred that the optimal charging mass of working fluid exists over m=8.9 g for H=10 mm.

4.2 Analytical solution

Figure 6 shows the axial distribution of pressure difference between liquid and vapor and capillary pressure for the operating temperature 293 K and the heat load 200 W. The difference of liquid pressure drops rapidly in an axial direction, whereas the vapor pressure drops slowly. The rapid drop of liquid pressure is due to the high friction of liquid through axially grooved wick and the slow drop of vapor pressure due to the low friction of vapor through a core of pipe.

Figure 7 shows the axial variations of the radius of curvature of liquid-vapor interface for the operating temperature 293 K. The radius of curvature of liquid-vapor interface approaches to half a width of groove $w/2$ at the end of evaporator and infinite at the end of condenser. The recession of interface to the groove bottom at the evaporator causes the charging mass

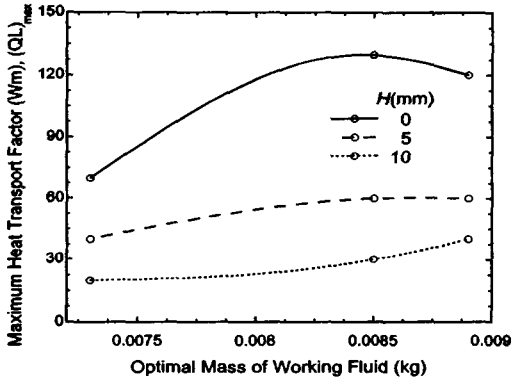

Fig. 5 Heat transport capacity versus the mass of working fluid charged for several elevations.

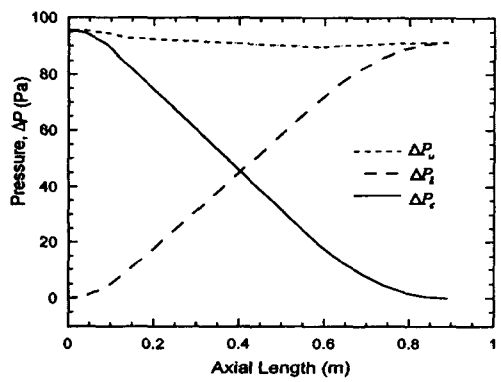

Fig. 6 Axial distributions of pressure at the operating temperature of 293 K and H= 0 mm.

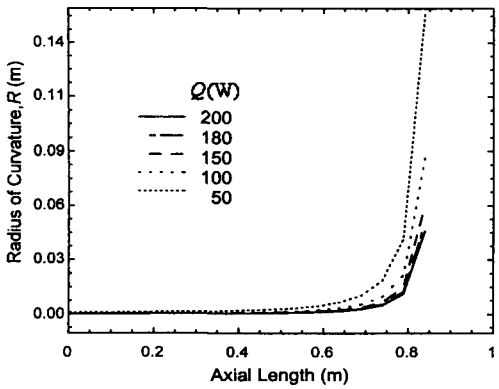

Fig. 7 Axial variation of curvature of radius at the operating temperature of 293 K and H=0 mm.

quantity of working fluid to be reduced. It can be found that the interface of liquid-vapor is more regressed to the bottom of groove with the heat load increasing. These results are in good agreement with that of Feldman et al.[9]

Figure 8 depicts the axial distribution of capillary pressure at the operating temperature 293 K with increasing the heat load imposed on the evaporator of heat pipe. The capillary pressure varied axially in a typical pattern of $\Delta P_c = \sigma/R$, which is large in the evaporator region and reduced rapidly in the condenser region. The capillary pressure difference induced by the evaporation of vapor at the evaporator becomes large with the heat load increasing. For the heat pipe used in this study, the maximum capillary pressure difference appears at the heat load of 200 W. For the condenser region of heat pipe, the capillary pressure difference approaches to zero and independent of heat load.

It is shown in Fig. 9 that experimental result is compared with that from analysis for the maximum heat transport capacity of heat pipe with the charging mass of working fluid at H=0 mm. m_0 and $(QL)_0$ denote the charging mass of working fluid and the maximum heat transport capacity of heat pipe, based on the model of Chi,[7] respectively. The normalized maximum heat transport capacity from $(QL)_0$ depends experimentally the normalized charging mass of working fluid by m_0. Solid and dotted lines denote the cubic spline fitting lines for experiment and analytical data, respectively. The maximum heat transport capacity is achieved analytically at the charging mass 8.5458 g and experimentally at the charging mass 8.5 g for the operating temperature 293 K. Experimental result for the charging mass of working fluid is therefore in good agreement with the analytical solution.

Otherwise, the analytical solution reveals that the maximum heat transport capacity of heat

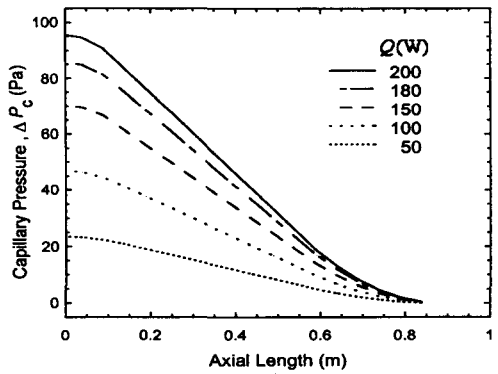

Fig. 8 Axial variations of capillary pressure at the operating temperature of 293 K and H=0 mm.

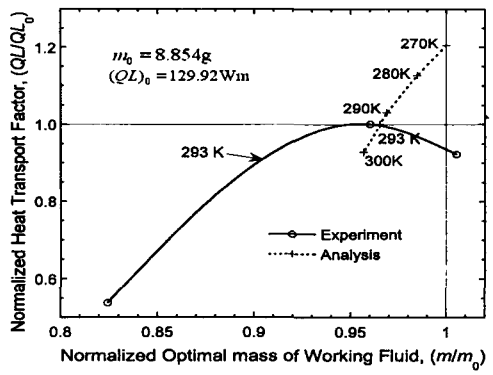

Fig. 9 Comparison of experimental and analytical results for the optimal mass of working fluid charged at H=0 mm.

pipe is reduced with the operating temperature increasing, owing to the property variation of the working fluid of ammonia corresponding to the operating temperature.[4]

In a result, it can be found that, for the maximum heat transport capacity of heat pipe with axially grooved wick, the optimal charging mass of working fluid is less than that from the analytical solution based on the simple model of Chi.[7]

5. Conclusions

An analytical and experimental study of the thermal performance of heat pipe with axially grooved wick is conducted to determine the optimal mass of working fluid for the maximum heat transport capacity. In this work, the optimal mass of working fluid was obtained by considering the recession of liquid-vapor interface of working fluid occurred in the evaporator region. Additionally, It was found that, from the analytical solution, the axial variation of capillary pressure, the radius of curvature and wetting angle of meniscus of liquid-vapor interface depend on the heat load imposed on the evaporator of heat pipe. Finally, the analytical results of the optimal mass of working fluid were in good agreement with those of the experimental mass of working fluid. It was found that the optimal charging mass of working fluid is 8.5 g for the heat pipe used in the work at the operating temperature 293 K.

Acknowledgement

This work was partially supported by the grants from the Brain Korea 21 project, NURI project, Research Center for Aircraft Parts Technology, and the Program for the Training of Graduate Students in Regional Innovation which was conducted by the Ministry of Commerce, Industry and Energy of the Korean Government.

References

1. Kemme, Josep E., Aug. 1, 1969, Heat Pipe Design Considerations, Report LA-4221-MS, of the Los Alamos Scientific Laboratory of the University of California, Los Alamos, N. Mex. (for presentation at the 11th Heat Transfer Conference, Aug. 3-6, 1969, Minneapolis, Minn.), pp. 1-8.
2. Tathgir, R. G. and Singth, G., 1984, Performance characteristics of a stainless steel gravity assisted grooved water heat pipe at low temperature, The Proceeding of 5IHPC Part I, pp. 18-23.
3. Ogushi, T. and Yanmanaka, G., 1986, Heat transfer performance of axial grooved heat pipes, Trans. JSME, No. 86-0252A, pp. 600-607.
4. Shin, D. Y., 1987, An Experimental Study on the Optimal Charge of Working Fluid for Heat Pipe, M.S. Thesis of Seoul National University.
5. Lee, W., Park, Y. J., Suh, J.-S. and Kim, M.-G., 1997, Analysis and experiment for thermal performance of grooved heat pipe, Proci. the Air-Conditioning and Refrigeration Engng 1997 Summer Annual Meeting, Vol. 2, pp. 512-517.
6. Park, Y. J., Kyun, W. S. and Suh, J.-S., 1998, Effects of the groove shape on the thermal performance of a axial groove heat pipe, Proci. the Air-Conditioning and Refrigeration Engng 1998 Winter Annual Meeting, Vol. 1, pp. 257-262.
7. Chi, S. W., 1976, Heat Pipe Theory and Practice, McGraw-Hill, New York.
8. Peterson, G. P., 1994, An Introduction to Heat Pipes, John Wiley & Sons, New York.
9. Feldman Jr. K. T. and Whiting, G. H., 1967, The heat pipe, Mechanical Engineering, pp. 30-33.
10. Ivanovskii, M. V., Sorokin, V. P. and Yogodkin, I. V., 1982, The Physical Principles of Heat Pipes, Clarendon Press, Oxford.